Andrea Belleri, Mauro Torquati, Alessandra Marini, Paolo Riva. 2017.
"Simplified building models as advanced seismic screening tools for steel industrial buildings". Journal of Constructional Steel Research, Vol. 138, pp. 51-64. DOI: 10.1016/j.jcsr.2017.06.027

Publisher's version:
https://doi.org/10.1016/j.jcsr.2017.06.027

Simplified building models as advanced seismic screening tools for steel industrial buildings

Andrea Belleri, Mauro Torquati, Alessandra Marini, Paolo Riva

Department of Engineering and Applied Sciences, University of Bergamo, Italy

Abstract

The present paper investigates the suitability of simplified building models to be used as advanced screening tools for the seismic vulnerability assessment of older industrial steel buildings. The considered buildings have been built before the enforcement of modern seismic codes and they are characterized by joints with low ductility and by the absence of capacity design provisions. In addition, such buildings, characterized by a wide plan extension, are typically part of large industrial areas. The complex geometry of the buildings makes the creation of a complete finite element model difficult. This is due to the high number of degrees of freedom and to the consequent high number of vibration modes to be included in a general response spectrum analysis. To overcome such limitations, simplified building models for advanced seismic screening are herein proposed and compared to traditional vulnerability procedures. Such procedures may be used for a first estimate of the seismic vulnerability of older and large industrial buildings, in order to identify and quantitatively rank seismic deficiencies before a detailed assessment. The validation shows that the investigated approaches are particularly suitable for seismic risk assessment of building portfolios and for providing a first estimate of the load demand in the elements of the lateral force resisting system.

Keywords:
Simplified building models; Seismic screening; Old steel buildings; Large industrial buildings;

1 Introduction

After the Emilia (Italy) earthquake in 2012, where many industrial buildings were damaged (Liberatore et al. 2013, Magliulo et al. 2014, Belleri et al. 2014 and 2015), a growing attention has been placed on existing plants. Old industrial buildings not designed following modern anti-seismic criteria were considered, both to preserve human life and to avoid the downtime and losses caused by possible future seismic events. Such buildings present a wide plan extension, a structural layout typical of the Italian pre- and post- World War II period, a general low ductility of the connections and the absence of capacity design provisions.

The main structural elements are typically riveted built-up members connected by means of bolted connections. Runway beams are placed in the longitudinal directions to support overhang cranes; these beams are typically composed of by truss members or by assembled I-shape beams. Due to the large distance between adjacent columns (> 20m), the bracing is provided by inclined elements connected to the crane runway beams or by stiffer columns in the longitudinal direction. In the transverse direction, the columns act as cantilever elements. The roof is supported by lattice beams spanning in the transverse direction, which are typically supported by lattice girders connecting adjacent columns or supported directly by the crane runway beams by means of vertical elements. The roof diaphragm action is provided by cross bracing spanning in the longitudinal and transverse direction. **Figure 1** shows some examples of typical members.

To assess the seismic vulnerability of existing buildings, reference can be made to the methodologies found in national and international building codes (D.M. 14/01/2008, EN 1998-3:2005, FEMA 356), which follow worldwide recognized seismic design methods and involve linear and non-linear procedures. The main target of such procedures is the definition of a building seismic vulnerability index, which is obtained by considering the overall behaviour of the structure and by comparing the seismic demand and capacity of the elements and the connections. However, the extensive plan dimension of the considered building typology requires much more effort for the creation of the finite element model compared to smaller buildings, due to the high number of

55 elements and associated degrees of freedom. This leads to a high number of vibration modes to be
56 considered and to a subsequent high computational demand. In addition, in the case of wide
57 industrial buildings, extensive industrial areas or large portfolios, seismic screening procedures are
58 more appropriate for a preliminary seismic risk assessment and management, as required in the
59 industrial and insurance fields. Therefore, simplified screening procedures are more appealing.

60 

61 

62 *Figure 1 – Examples of typical details of old industrial buildings.*

63 At this regard, it is worth referring to the work of Petruzzelli (2013) who suggested tackling this
64 problem at different scales as a function of the number of considered buildings. A “large-scale”,
65 involving hundreds or thousands of buildings, in which only a general and preliminary assessment
66 is carried out by comparing the seismic capacity of the building with the seismic demand according

67 to the building code enforced at the time of construction. In the case of sites which were not
68 classified as seismic-prone in the past, it is possible to compare the actual seismic demand with the
69 wind load demand at the time of construction. The main purpose of the "large-scale" approach is to
70 act as a decision-making tool enabling the rational ranking of priorities, identify needs of more
71 advanced analyses, or to plan possible retrofit interventions and mitigation measures. Such an
72 approach could be categorized as a type of "seismic screening". A "meso-scale", involving
73 buildings of a specific industrial area, in which a fragility curve is defined for each structure or class
74 of structures in the portfolio; this allows evaluating the expected seismic losses. The fragility curves
75 could be appositely developed or inherited from past projects (Hazus, 2003; Pitilakis et al., 2013). A
76 "site-specific scale" involving the analysis of a single building, in which conventional seismic
77 analyses, as non-linear dynamic analyses, are carried out on a complete model of the building to
78 obtain the failure probability (Petruzzelli et al. 2012a, 2012b).
79 The present paper investigates two simplified building models suitable for a first estimate of the
80 seismic vulnerability of the industrial buildings under investigation. In both cases, linear elastic
81 analyses are conducted. The first approach considers planar models of the building and it requires a
82 limited number of elements. The procedure allows estimating the load demand on the elements of
83 the lateral force resisting system, namely vertical and horizontal bracing. The second approach
84 considers a three-dimensional model of the building. Auxiliary elements with equivalent stiffness
85 and mass are included in the model to significantly reduce the number of elements, degrees of
86 freedom and, consequently, modes of vibration required in a response spectrum analysis. Following
87 the categorization of Petruzzelli (2013), such approaches may be included in the "site-specific
88 scale", because they require the knowledge of specific buildings. Nonetheless, the proposed
89 simplified building models, allowing for an advanced seismic screening by means of linear
90 analyses, do not require the definition of computational-demanding fragility curves and therefore
91 they could be adopted at the "meso" and "large" scale, especially in the case of recurrent structural
92 layouts and recurrent details in different geographical areas.

2 *Seismic screening and vulnerability assessment of existing industrial buildings*

2.1 Seismic screening

Seismic screening is a preliminary structural assessment tool. It has the advantage of highlighting potential seismic deficiencies and it is adopted both to rank the seismic vulnerability of buildings among a portfolio and to get a preliminary estimate of the seismic risk of a given building. FEMA 154 and ASCE/SEI 41 are examples of seismic screening procedures.

FEMA 154 provides a procedure for a rapid visual screening and ranking of buildings in seismic prone areas. The procedure is mainly intended for relative risk comparison among large groups of buildings and for prioritization of further studies and analyses. However, such procedure can also be used for a quick assessment of the potential seismic performance of a given building. A visual inspection of the building is the first step required by the procedure. The seismic-force-resisting system and any characteristic that might influence the expected seismic performance are identified. Given the building structural system, a score is assigned based on the level of seismicity of the region in which the building is located. Such score reflects the likelihood that a typical building of a given typology would sustain damage to such an entity beyond which life safety begins to become a serious concern. The score is then modified based on building attributes or site features that may increase or decrease the seismic vulnerability, such as the number of storeys, vertical or horizontal irregularities and the soil type. Finally, a structural score for the building is obtained, ranging between 0 and 7. The highest scores correspond to a better expected seismic performance.

ASCE/SEI 41 defines a three-tiered process for seismic evaluation. Each successive tier is characterized by an increased effort and by a greater confidence in the identification and confirmation of any seismic deficiency. Tier-1 regards the seismic screening, Tier-2 deals with a deficiency-based evaluation procedure and Tier-3 refers to a systematic evaluation procedure.

Tier-1 and Tier-2 are intended for buildings belonging to defined typologies referred to as "common building types", but are inapplicable to the structural typology under investigation. Tier-3 is intended to cover all other building typologies, thus applicable to the investigated typology but

119 requiring refined analyses. The literature survey emphasises the need for simplified evaluation
120 procedures to be referenced to in the case of large industrial buildings.

121 Similarly to FEMA 154, Tier-1 requires the completions of quick checklists for each building
122 type, including information on the presence of a complete load path for inertia loads, the
123 redundancy of the lateral force resisting system, the possible influence of adjacent buildings, the
124 presence of weak or soft storeys, the number of vertical or horizontal irregularities, the liquefaction
125 susceptibility of the soil, the foundation configuration, and the type of non-structural components
126 among others. After the collection of the data from all the checklists, the building deficiencies are
127 summarized and the need for further analyses is highlighted. In Tier-2, all the potential deficiencies
128 identified in Tier-1 are evaluated. Additional analyses are carried out to confirm each deficiency or
129 to demonstrate the adequacy of the structure. Where required, the analysis of the seismic-force-
130 resisting system shall be based on linear static or linear dynamic procedures. Tier-2 considers the
131 evaluation of the potential deficiencies identified in the screening phase (Tier-1).

132 Other tools that might be adopted as seismic screening make use of fragility curves. At this
133 regard, the project SYNER-G (Pitilakis et al., 2013) developed a series of fragility curves to be used
134 in risk assessment procedures. The project focused on the definition of harmonized typologies and
135 taxonomies for European buildings, lifeline networks, transportation infrastructures, utilities and
136 critical facilities. This approach has the advantage to provide a quick reference value for the seismic
137 vulnerability. The high scatter of the results and the impossibility of detecting the most vulnerable
138 elements represent the disadvantages of this methodology. The aforementioned project does not
139 consider steel industrial buildings specifically.

140 **2.2 Seismic vulnerability assessment**

141 The existing seismic vulnerability assessment procedures (as in D.M. 14/01/2008, EN 1998-
142 3:2005, FEMA 356) can be distinguished into linear and non-linear. Linear procedures can be
143 subdivided into “linear static” and “linear dynamic” analyses. Non-linear procedures are
144 represented by “non-linear static” and “non-linear dynamic” analyses.

As regards linear procedures, linear static methods are the simplest way to estimate the seismic response, although their applicability to the considered industrial buildings is generally limited to buildings regular in elevation. In the structural typology under investigation, the lateral stiffness of the structural element below the overhead crane is typically much higher compared to the elements supporting the roof structure. Linear dynamic methods, i.e. response spectrum analyses, allow considering and combining different vibration modes (Roeder et al., 2002). The linear dynamic approach follows an elastic analysis in which a behaviour factor is introduced to account for structural non-linearity as plastic hinge formation. The main issue of this method is related to the choice of the behaviour factor, especially in the case of systems with limited ductility.

As regards non-linear procedures, non-linear static methods consider the application of a lateral force distribution with increasing magnitude to obtain the building capacity curve (typically base shear versus roof displacement). Examples of non-linear static methods, i.e. pushover analyses, are found in Chopra and Goel (2002), Kreslin and Fajfar (2011), Nguyen et al. (2010), Lopez-Almansa and Montana (2014), and Wijesundara et al. (2014) among others. The capacity curve is converted into an equivalent single degree of freedom system curve and compared to the demand spectrum. In the case of non-linear dynamic methods, i.e. time history analyses, the material non-linearity and the higher modes' contribution are directly included by applying an acceleration history at the base of the structure, often by means of incremental dynamic analysis (Vamvatisikos and Cornell, 2002).

Taking as reference EN 1998-3:2005, the knowledge level achieved by the engineer at the beginning of the assessment procedure needs to be accounted for when dealing with the seismic assessment of existing buildings. The knowledge level is associated with the investigation of the construction documents, the field surveying and the diagnostic campaigns. Therefore, it is bound to aspects related to the structural system identification, the properties and details of the structural elements and the mechanical properties of the materials. For instance, in the considered steel buildings the connections between elements play a significant role, as they determine the difference between ductile and fragile behaviour of the structure during a seismic event. Three knowledge

levels are introduced (EN 1998-3:2005) as a function of the amount of data acquired, namely "limited", "normal" and "full" knowledge level. Once the resisting scheme is identified, the appropriate level is determined by means of surveys on the geometrical properties of the structural elements, on the details of the connections and on the mechanical properties of the materials. Such information could be obtained from available documentation, field investigation and from in-field or laboratory tests. A confidence factor is associated to each knowledge level: 1.35, 1.20 and 1.00 for limited, normal and full knowledge level, respectively. The seismic capacity of the members is finally evaluated considering the mean values of the material properties divided by the confidence factor and by the material partial safety factor γ_M. The material properties are reduced by the sole confidence factor in the case of ductile members and linear analyses.

As mentioned before, the typical assessment procedures require computational-demanding analyses, due to the extensive plan dimensions of the considered building typology and to the high number of elements because of lattice/truss girders and columns. In the following paragraphs, two simplified building models are presented: Simplified Planar Model (SPM) and Equivalent Elements Model (EEM). The models are implemented into linear elastic procedures to provide advanced screening tools for a first estimate of the seismic vulnerability of the buildings being examined. Both procedures allow for a reduction of the number of elements to be used in the finite element models. Consequently, a significant reduction of the computational effort and a faster estimation of the seismic demand in the lateral force resisting system are obtained. As screening tools, these procedures do not substitute a more detailed assessment and the confirmation of potential seismic deficiencies.

2.3 Procedure 1: Simplified Planar Model (SPM)

In the first approach, the seismic loads acting on the lateral force resisting system are obtained from response spectrum analyses on simplified finite element planar models. Two separate analyses are carried out considering the building principal directions. In industrial buildings, the typical structural layout consists of uninterrupted bays in the longitudinal directions to accommodate

197 production lines and overhead cranes. In this direction the lateral load resisting system is provided
198 by ad-hoc bracing elements or by laced or battened columns with increased stiffness. In the
199 transverse direction the static scheme is either a portal frame with rigid beam-to-column joints or
200 cantilever columns pin-connected to the supported beams.

201 Starting from the longitudinal direction (braced direction), a simplified planar model is defined
202 including the braces and the connected elements (**Figure 2a**), such as the crane runway beams and
203 the beams supporting the roof trusses. Only half length of the connected beams and girders is
204 included in the model due to the assumption of a point of contra-flexure at the beam centre because
205 of seismic actions; for the same reason, vertical rollers are introduced as boundary conditions at the
206 ends of the half-length beams. The column tributary mass m_c is placed directly in the model and it
207 corresponds to the area delimited by the centre-to-centre distance between adjacent columns. The
208 lateral stiffness of the columns along the considered longitudinal alignment (k_{1_L}, k_{1_R}, k_{2_L}, k_{2_R}) and
209 the corresponding mass (m_{bot_L}, m_{bot_R}, m_{top_L}, m_{top_R}) are lumped into springs and point masses at
210 each side of the simplified planar model, respectively. The values of k_1 and k_2 are obtained from a
211 finite element model representing a standard column. k_{1_L} and k_{1_R} are the total lateral stiffness
212 associated to the lower part of all the columns placed respectively on the left and right side of the
213 braced system. The stiffness of a single column is obtained from applying a horizontal unit
214 displacement at a height corresponding to h_1 (**Figure 2**). The corresponding base shear represents
215 directly the unit stiffness. k_{2_L} and k_{2_R} are the total lateral stiffness associated to the upper part of
216 all the columns placed respectively on the left and right side of the braced system. The stiffness of
217 the upper portion of a single column is obtained from applying a horizontal unit displacement at a
218 height corresponding to h_2 while preventing horizontal displacements at the quote h_1 (**Figure 2**).
219 The shear in the upper portion of the single column represents directly the unit stiffness. m_{bot_L} and
220 m_{bot_R}, are the masses of the rest of the structure related to the bottom portion of the system
221 (corresponding to h_b in **Figure 2**), left and right side respectively. m_{top_L}, and m_{top_R} are the masses

of the rest of the structure related to the upper portion of the system (corresponding to h_t in **Figure 2**), left and right side respectively.

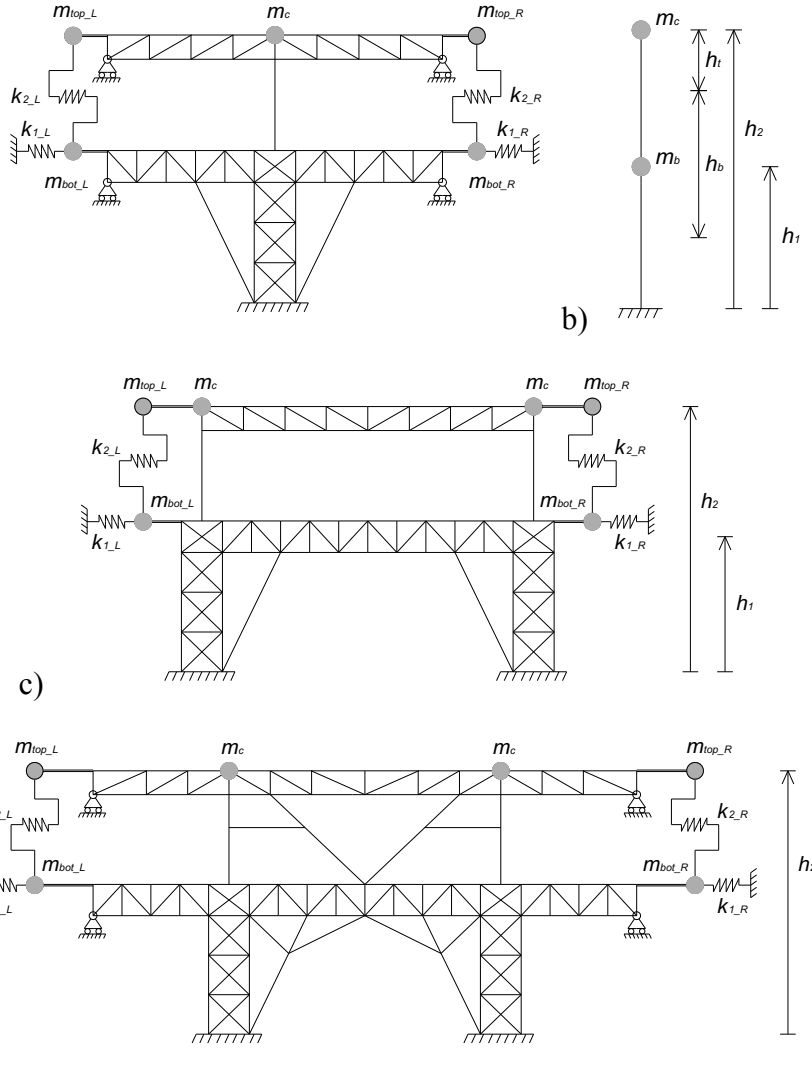

Figure 2 – Simplified planar model (SPM) including the braces and the connected elements: a) in-plane and b) out-of-plane; c) d) additional examples of simplified planar models. Note: m_{bot_L} (m_{bot_R}) is the sum of the left (right) masses at the crane runway beam level; m_{top_L} (m_{top_R}) is the sum of the left (right) masses at the roof level; m_c (m_b) is the tributary mass of the considered column (crane girder); k_{1_L} (k_{1_R}) is the stiffness of the left (right) columns; k_{2_L} (k_{2_R}) is the stiffness of the left (right) top portion of the columns;

The transverse direction is treated similarly. In the case of a static scheme with cantilever columns pin-connected to the roof truss, only a single column with the corresponding tributary mass is considered in the simplified model (**Figure 2b**). The response spectrum analyses in both directions provide directly the load demand on the elements of the vertical lateral force resisting system. The tributary mass at the roof level corresponds to the roof mass divided by the number of column alignments. For other bracing systems, the same procedure can be adopted to determine all

the property of the simplified model and to calculate the seismic loads acting on the structural elements. **Figure 2c** and **Figure 2d** show two examples of simplified planar models.

The load demand in the horizontal components of the lateral force resisting system, i.e. the bracing elements of the roof diaphragm, is evaluated treating the roof bracing in the longitudinal and transverse directions as single beams on elastic supports (**Figure 3**). The same procedure described in the next paragraph is adopted to include both flexural and shear deformation in the represented beams. Translational springs are placed at the column joints in the transverse direction (k_y) and in correspondence to the longitudinal bracing alignment (k_x). Rotational springs are placed at the intersections between the longitudinal and transverse bracing to account for the rotational stiffness (k_{rot}) of such joint. The inertia loads p_x and p_y are obtained considering the shear demand in the upper portion of the columns, in the longitudinal and transverse direction respectively.

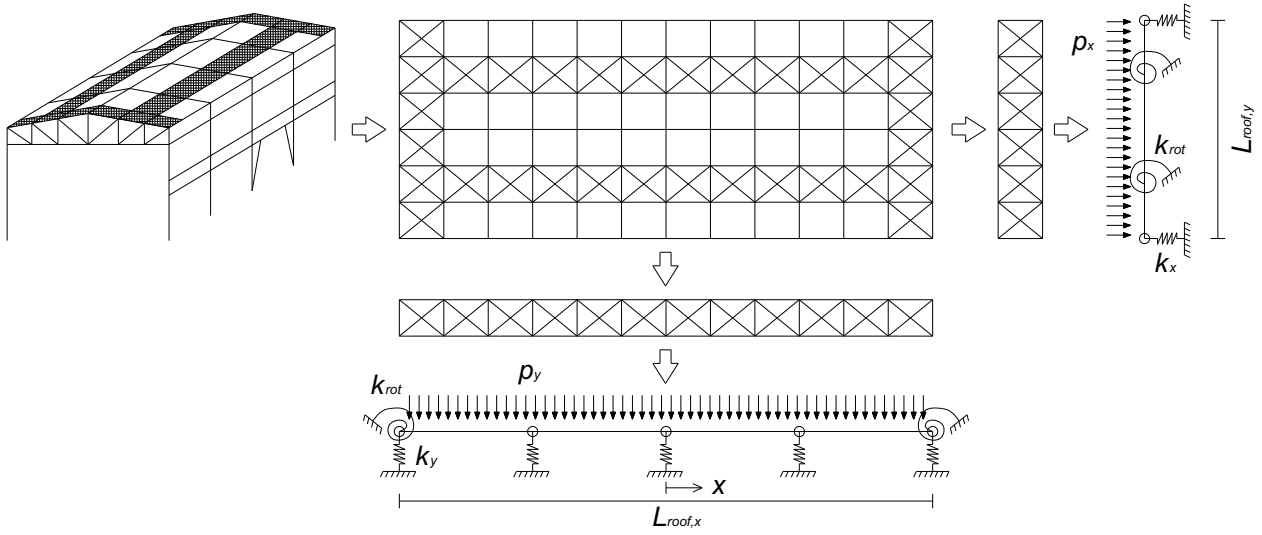

Figure 3 – Simplified evaluation of the roof bracing system for the simplified planar model (SPM).
Note: k_x (k_y) is the translational stiffness in the x (y) direction; k_{rot} is the rotational stiffness due to the framing of orthogonal bracing; p_x (p_y) is the equivalent distributed load in the x (y) direction.

2.4 Procedure 2: Equivalent Elements Model (EEM)

This section provides the theoretical background associated to the derivation of simplified formulations for built-up elements with lacings and battenings. The procedure is based on the equivalent web area method which was specifically derived to account for the shear stiffness of open web elements (Ballio and Mazzolani, 1983). The idea behind the method is to find an

equivalent I-beam with the same flexural and shear stiffness of the considered member. The procedure is valid for members with parallel chords. The properties of the equivalent I-beam are: same cross-section height as the original member; area of each I-beam flange equal to the area of each chord; web with equivalent thickness. Therefore, the flexibility of the equivalent I-beam could be seen as the sum of two contributions: the flexural flexibility of an ideal beam with second moment of inertia provided by a point mass lumped at each chord centroid, and the shear flexibility associated to an equivalent web plate providing the same shear stiffness of the original built-up member. In the case of chord elements with different cross-section, an equivalent area is evaluated as the weighted mean of the area of each element considering the element length as weight. The evaluation of the equivalent area is carried out independently for the top and bottom chord, leading respectively to A_{ct} and A_{cb}.

To obtain the web thickness of the equivalent I-beam it is worth distinguishing between laced and battened elements. In both cases, the shear displacement of the built-up element is assumed equal to the shear displacement of a plate with the same geometry and equivalent web thickness (**Figure 4**). In the case of laced built-up elements, the area A_w of the equivalent web plate is obtained from equating the shear displacements of the plate to the shear displacement of the built-up element. The latter is associated with the lengthening of diagonal d_1 and shortening of diagonal d_2 (**Figure 4**):

$$A_w = \frac{E}{G} \frac{\cot\theta_1 + \cot\theta_2}{\frac{1}{A_{d1}\sin^3\theta_1} + \frac{1}{A_{d2}\sin^3\theta_2}} \tag{2}$$

E and G are the steel Young's and shear modulus, respectively; A_{d1} and A_{d2} are the cross-section area of the diagonal elements d_1 and d_2, with inclination θ_1 and θ_2 with respect to the horizontal axis, respectively. In the case of built-up members with diagonal elements d_1 with different cross sections, the mean cross-section area is considered; the same applies for diagonal elements d_2.

The equivalent I-beam is therefore characterized by a top flange with area A_{ct}, a bottom flange with area A_{bt} and a web with area A_w. To account for the variation of weight arising from A_w, the following equivalent density (ρ_{eq}) is considered as a function of the steel density (ρ_{steel}):

$$\rho_{eq} = \rho_{steel} \frac{A_{ct} + A_{cb} + A_{d1}\frac{L_{d1}}{L_0} + A_{d2}\frac{L_{d2}}{L_0}}{A_{ct} + A_{cb} + A_w} \tag{3}$$

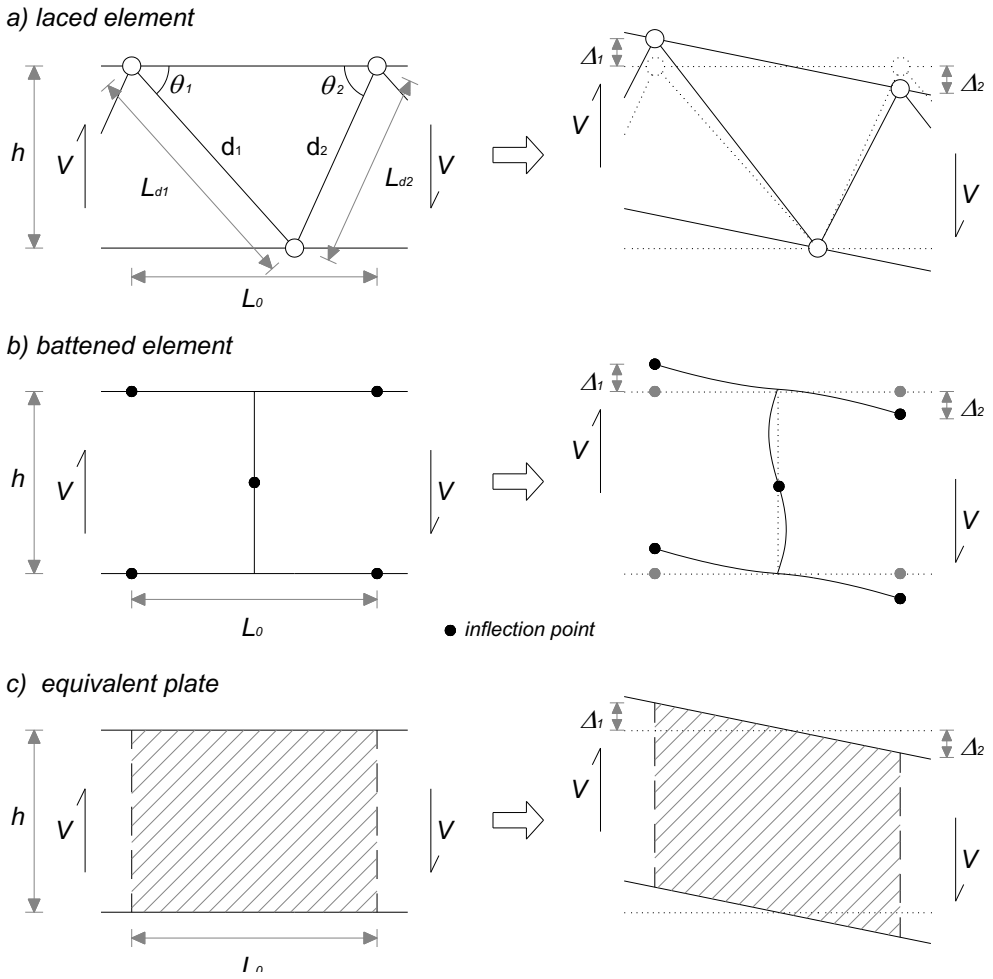

Figure 4 – Shear displacement for built-up elements and equivalent plate

In the present work, the flange dimensions are selected in order to provide the same out-of-plane stiffness of the original member. The equations providing the flange width (B) of the I-beam are

$$B_t = \sqrt{12\frac{I_{zz\_ct}}{A_{ct}}}\ ;\ B_b = \sqrt{12\frac{I_{zz\_cb}}{A_{cb}}} \tag{4; 5}$$

where I_{zz_ct} and I_{zz_cb} are the out-of-plane second moment of inertia of the top and bottom chord, respectively. The flange thickness is obtained from dividing the area of each flange by its width.

A further approximation adopted herein is providing the same dimension for the top and bottom flanges of the I-beam. This is accomplished by replacing A_{ct} and A_{cb} with $A_c=(A_{cb}+A_{ct})/2$. **Eqn.4** and **Eqn.5** are substituted with:

$$B = \sqrt{12\frac{I_{zz\_ct} + I_{zz\_cb}}{2A_c}} \tag{6}$$

The flange thickness is directly A_c/B. Such approximation leads to a stiffness overestimation of less than 13% in the case of a cross-section area of one chord equal to twice the area of the other chord, therefore representing a reasonable approximation.

In the case of battened elements subjected to shear, inflection points are assumed at the mid point of each batten and at each chord in correspondence to half distance between adjacent battens (**Figure 4**). The shear stiffness of the battened elements is provided by three contributions: the flexural stiffness of the chord, the flexural stiffness of the batten and the shear stiffness of the batten. The area A_w of the equivalent web plate is:

$$A_w = 12\frac{E}{G}\frac{1}{\frac{L_0^2}{2I_c} + \frac{L_0 \cdot h}{I_b}} \tag{7}$$

where I_c and I_b are the second moment of inertia of the chord and the batten, respectively. I_c is taken as the mean between top and bottom chord second moment of inertia. The flange width and thickness of the equivalent I-beam are obtained as in the case of laced elements.

Once the analyses have been carried out, the axial load acting on the chord elements of the original structure are determined as the sum of the axial load of the equivalent element and the load associated with the bending moment (i.e. bending moment of the equivalent element divided by the equivalent element height). The axial load acting on the web elements of the original structure is taken directly from equilibrium with the shear load acting on the equivalent element.

The equivalent area method can also be applied to roof bracing members, truss roof beams, laced columns, and battened columns among others. In the case of columns with a general and not repetitive layout (lower portion of **Figure 5a**), or in the case of columns with two consecutive

element sets (**Figure 5a**), it is possible to define equivalent elements. The following procedure applies. A given force (F) is placed at the top of the laced portion of the column (**Figure 5b**) and the resultant top displacement (v) and rotation (v') are recorded. The flexural stiffness (I) and the web area (A_w) of the equivalent beam element are obtained from equating v and v' with the corresponding displacement and rotation associated with a uniform cantilever beam:

$$\begin{cases} v = \dfrac{FH}{GA_w} + \dfrac{FH^3}{3EI} \\ v' = \dfrac{FH^2}{2EI} \end{cases} \Rightarrow \begin{cases} I = \dfrac{FH^2}{2E}\dfrac{1}{v'} \\ A_w = \dfrac{3FH}{G\left(3v - 2Hv'\right)} \end{cases} \tag{8}$$

where H is the height of the considered laced part of the column. This evaluation is carried out for both the in-plane and out-of-plane directions, leading respectively to A_{wy}, I_y and to A_{wz}, I_z. An equivalent I-beam is defined with flange dimensions (t_f, B) and web dimensions (t_w, h). The relationships between the I-beam dimensions and A_{wy}, I_y, A_{wz}, I_z are:

$$A_{w\,y} = t_w h; \quad A_{w\,z} = 2t_f B; \quad I_y = 2Bt_f\left(\frac{h}{2}\right)^2 + \frac{t_w h^3}{12}; \quad I_z = 2\frac{t_f B^3}{12} \tag{9; 10; 11; 12}$$

which leads to the equivalent I-beam dimensions:

$$t_f = \sqrt{\frac{A_{w\,z}^{\,3}}{48 I_z}}; \quad B = \frac{A_{w\,z}}{2t_f}; \quad h = \sqrt{\frac{12 I_y}{6Bt_f + A_{w\,y}}}; \quad t_w = \frac{A_{w\,y}}{h} \tag{13; 14; 15; 16}$$

The density of the equivalent I-beam leading to the same mass of the original structure (m_{real}) is:

$$\rho_{eq} = \frac{m_{real}}{H\left(2Bt_f + t_w(h - t_f)\right)} \tag{17}$$

In the case of columns with two consecutive element sets, a rotational spring is added (**Figure 5d**) to account for the flexural and torsion stiffness (i.e. in-plane and out-of-plane rotation) of the transverse beam (**Figure 5a**). The spring stiffness (k_s) is evaluated applying a bending moment (M) at the top of the transverse beam (**Figure 5b**) of the original structure and of the equivalent beam just found. The spring stiffness is $k_s = M/(v'_{real} - v'_{eq})$, where v'_{real} and v'_{eq} are the top rotation of the original structure and of the equivalent beam, respectively. The same procedure

is adopted to evaluate the spring stiffness for out-of-plane loading. It is worth noting that the column in **Figure 5** refers to the column shown in the last picture of **Figure 1**.

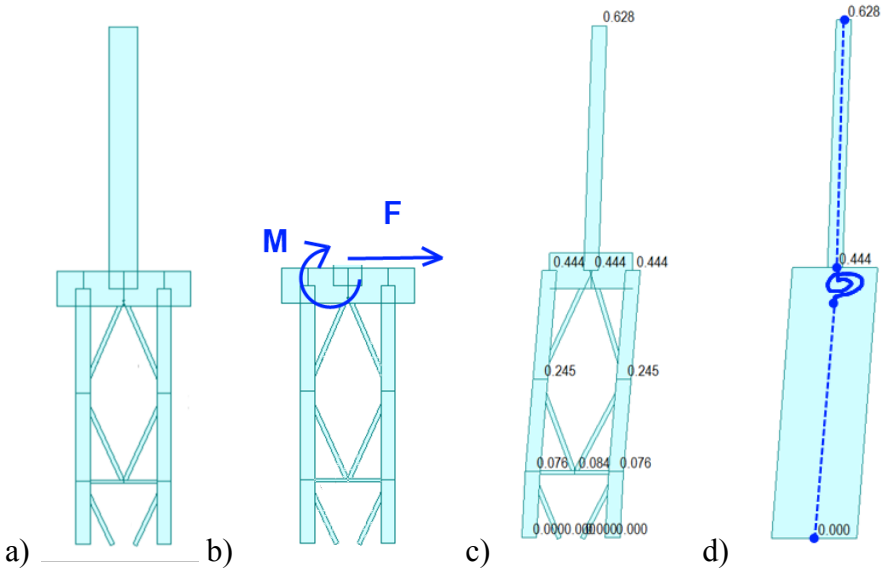

Figure 5 – Equivalent element in the case of columns with two consecutive element sets. Note: the column refers to the last picture in Figure 1 c) and d) shows the results (mm) of the proposed procedure in the case of a reference column with F=10kN and M=50kNm.

To further reduce the number of elements, equivalent plates are included in the roof to substitute the purlins between adjacent portals. The equivalent plates have the same axial stiffness and mass of the substituted purlins. The shear stiffness is set to zero, being the purlins pin-connected to the supporting elements. It is worth noting that such plates are not used to substitute the elements of the roof bracing system. **Appendix A** provides considerations on the influence of buckling in roof truss elements as a result of seismic loads.

3 Validation of the investigated procedures

The validation of the proposed SPM and EEM building models is carried out in two steps: the first step considers regular buildings as representative of portions of a typical industrial steel building; in the second step a wider and plan-irregular building is analysed. All the finite element analyses are carried out with the software MidasGen (2012). Once the loads on the elements have been determined, the comparison between the demand and the capacity can be performed. This comparison needs to be carried out both for elements and for joints, particularly in the case of joints

with low ductility and fragile failure, as it is the case of buildings built before modern seismic regulations. It is important to note that the deterioration of material conditions in old industrial buildings could further reduce the capacity of both members and joints. In the presence of low ductility joints and material deterioration further investigation is required.

For both procedures, P-Delta effects are considered through an amplification factor $1/(1-\theta)$, where θ is the stability index, defined as the ratio between second-order moment and first-order moment (AASHTO, 2009; EN 1998-1; BSSC, 2003).

3.1 Industrial building with regular plan extensions

The considered buildings are characterized by 6 bays with a span of 25m in the longitudinal direction (X in **Figure 6**) and by 1 and 3 portals of 30m span, respectively, in the transverse direction (Y in **Figure 6**). The columns, 14.5m high, present portions with different properties in terms of strength and stiffness. The discontinuity corresponds to the overhead crane. The lower part is a built-up laced member with 2 I-shape beams as chords and L-shape beams as laces. The upper part is a single I-shape element supporting the roof beam. 2 of such columns act as the bracing system for the horizontal loads in the X-direction; therefore, bigger elements are present.

The crane runway beams are made by weld assembled I-shape elements connected to the columns with a hinge constraint. The roof is composed by I-shape purlins and L-shape diagonal elements; the latter identify 4 roof beams in each bay which gather and transfer the roof seismic loads to the top of the columns. The roof is supported by truss beams made by box elements. The influence of roof sheeting and side cladding is not considered in the analyses.

The results obtained with the proposed simplified SPM and EEM approaches are compared with those obtained by means of a complete finite element model (CM). **Figure 6** shows the models adopted in the analyses. The detail of the members and the corresponding equivalent elements adopted in the EEM procedure are provided in **Appendix B**. The comparison between the different models is presented in the following tables. **Table 1** and **Table 2** show the results in terms of modal

properties. **Table 3** and **Table 4** report the maximum displacements and maximum loads in the main members of the bracing system.

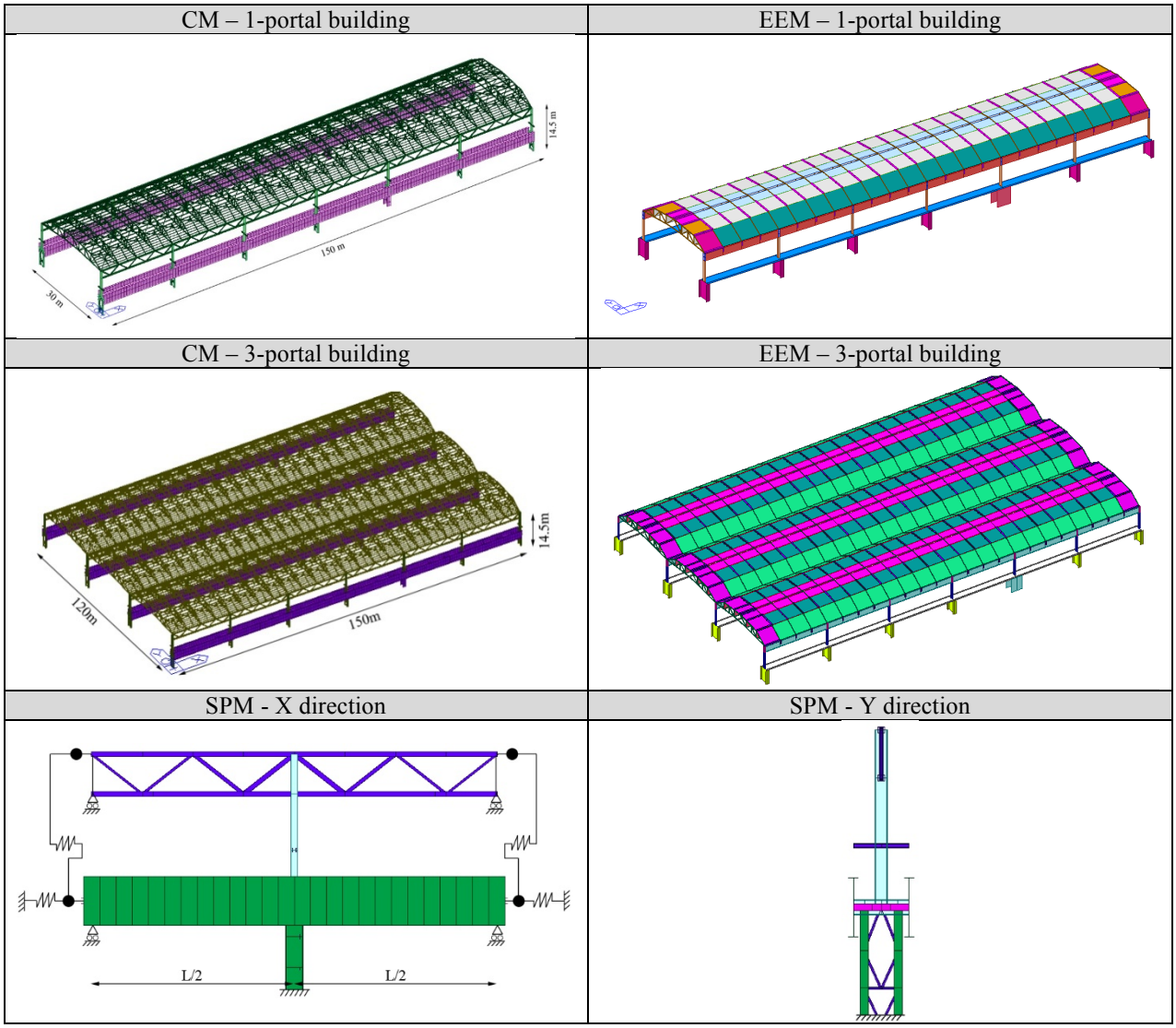

Figure 6 – Representation of the different models adopted
Note: CM = complete model; SPM = simplified planar model; EEM = equivalent elements model.

Table 1 – Comparison of modal properties; 1-portal building

Parameter		CM	SPM	SPM – CM relative error (%)	EEM	EEM – CM relative error (%)
1° mode – X-dir	Period (s)	1.39	1.29	**-7.2**	1.36	**-2.2**
	Modal participation mass (%)	46.2	46.7	+1.1	49.8	+7.8
1° mode – Y-dir	Period (s)	0.83	0.85	+2.4	0.84	+1.2
	Modal participation mass (%)	47.5	44.9	**-5.5**	50.1	+5.5
2° mode – X-dir	Period (s)	0.29	0.28	**-3.4**	0.28	**-3.4**
	Modal participation mass (%)	50.1	52.8	+5.4	50.1	0.0
2° mode – Y-dir	Period (s)	0.22	0.16	**-27.3**	0.19	**-13.6**
	Modal participation mass (%)	40.9	52.6	+28.6	33.6	**-17.8**

Table 2 – Comparison of modal properties; 3-portal building

Parameter		CM	SPM	SPM – CM relative error (%)	EEM	EEM – CM relative error (%)
1° mode – X-dir	Period (s)	1.63	1.56	**-4.3**	1.60	**-1.8**
	Modal participation mass (%)	52.8	55.5	+5.1	56.6	+7.2
1° mode – Y-dir	Period (s)	0.97	1.04	+7.2	0.96	**-1.0**
	Modal participation mass (%)	54.5	53.5	**-1.8**	57.8	+6.1
2° mode – X-dir	Period (s)	0.29	0.28	**-3.4**	0.29	0.0
	Modal participation mass (%)	44.0	44.0	0.0	33.83	**-23.1**
2° mode – Y-dir	Period (s)	0.21	0.16	**-23.8**	0.19	**-9.5**
	Modal participation mass (%)	17.1	44.4	+159.6	14.4	**-15.8**

Table 3 – Comparison of global displacements and maximum loads in the main members; 1-portal building

Parameter	CM	SPM	SPM – CM relative error (%)	EEM	EEM – CM relative error (%)
Horizontal global reaction X-dir (kN)	866.1	902.0	+4.1	832.3	**-3.9**
Horizontal global reaction Y-dir (kN)	776.4	886.4	+14.2	751.3	**-3.2**
Global displacement X-dir (mm)	43	38	**-11.6**	42	**-2.3**
Global displacement Y-dir (mm)	33	25	**-24.2**	33	0.0
Max. shear (X-dir) on bracing column (kN)	352.6	355.4	+0.8	341.1	**-3.3**
Max. shear (Y-dir) on bracing column (kN)	85.7	83.2	**-2.9**	83.5	**-2.6**
Max. shear (X-dir) on standard column (kN)	13.8	16.0	+15.9	13.1	**-5.1**
Max. shear (Y-dir) on standard column (kN)	80.3	72.0	**-10.3**	81.4	+1.4
Max. load in bracing column chord (kN)	354.4	314.7	**-11.2**	388.5	+9.6
Max. load in bracing column diagonal (kN)	81.9	73.0	**-10.9**	101.2	+23.6

Table 4 – Comparison of global displacements and maximum loads in the main members; 3-portal building

Parameter	CM	SPM	SPM – CM relative error (%)	EEM	EEM – CM relative error (%)
Horizontal global reaction X-dir (kN)	1765.6	1834.4	+3.9	1718.3	**-2.7**
Horizontal global reaction Y-dir (kN)	1610.2	1834.4	+13.9	1590.0	**-1.3**
Global displacement X-dir (mm)	53	45	**-14.6**	52	**-1.9**
Global displacement Y-dir (mm)	36	34	**-5.1**	35	**-2.0**
Max. shear (X-dir) on bracing column (kN)	369.6	361.4	**-2.2**	361.2	**-2.3**
Max. shear (Y-dir) on bracing column (kN)	88.8	85.6	**-3.6**	88.7	**-0.1**
Max. shear (X-dir) on standard column (kN)	14.2	16.3	+14.8	13.7	**-3.5**
Max. shear (Y-dir) on standard column (kN)	81.8	74.6	**-8.8**	84.6	+3.4
Max. load in bracing column chord (kN)	445.6	403.6	**-9.4**	434.9	**-2.4**
Max. load in bracing column diagonal (kN)	84.8	91.9	+8.4	107.7	+27.0

Table 1 and **Table 2** show a general good correspondence on the first mode of vibration in both directions (relative error being less than 8%). Higher differences arise in the second mode of

vibration (Y-dir) for both EEM and SPM. **Table 3** and **Table 4** show a good correspondence on the maximum horizontal global reaction, with a slight overestimation (14.2%) in the Y-dir for SPM. EEM provides the best global displacement predictions. Both SPM and EEM provide a good estimate of the shear in the bracing columns, while for standard columns the relative error in SPM is less than 16%. As regards the elements of the bracing column, SPM provides a slight underestimation of the axial load on both chord and diagonal elements (relative error less than 12%), while EEM provides an overestimation of the results (maximum relative error less than 27%). The differences between 1-portal and 3-portal buildings are limited.

As regards the roof bracing system, EEM allows for a direct provision of the loads in the bracing elements. In SPM, the loads in the roof bracing system can be derived according to the scheme depicted in **Figure 7**. Two types of beams (Beam 1 and Beam 2) are identified as part of the roof bracing system in the longitudinal and transverse direction, respectively. The roof corresponding to each portal is considered separately (i.e. 1 roof for the 1-portal building and 3 separate roofs for the 3-portal building). The columns are treated as elastic supports for the beams. The joint region between Beam 1 and Beam 2 is responsible for the rotational stiffness at each beam end (k_{rot}). The loads p_x and p_y (**Figure 7**) are obtained from the equilibrium with the shear values in the columns.

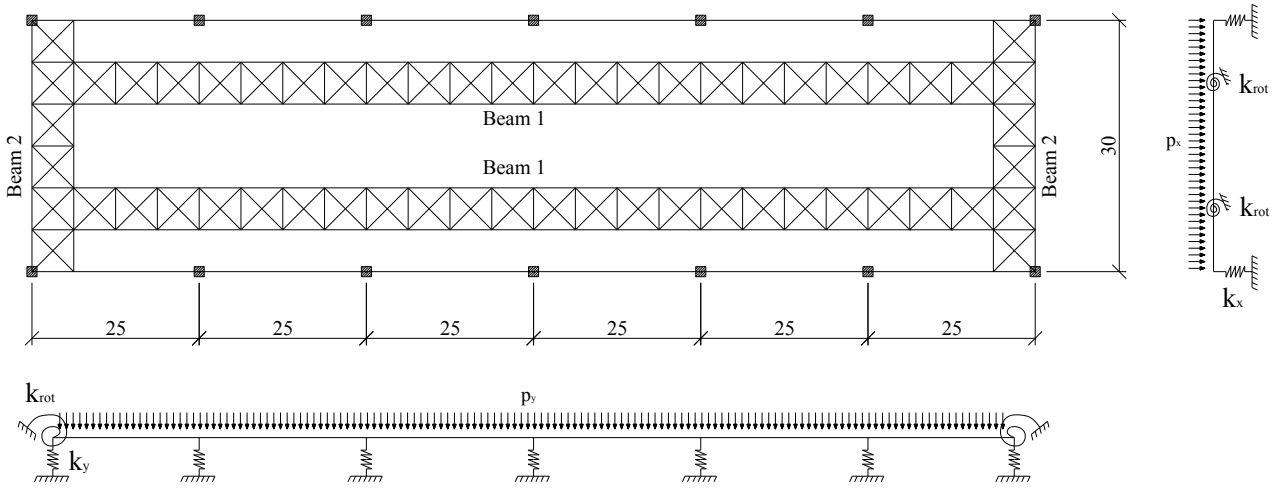

Figure 7 – Roof scheme adopted in SPM.
Note: dimensions in m.

Table 5 and **Table 6** show the maximum axial loads acting on diagonals and purlins of the roof bracing system for the considered models. The results show a general overestimation of the loads in the bracing system particularly for the transverse direction of SPM. **Table 7** shows the ratio between simplified and complete model in terms of number of elements, nodes, supports, required modes of vibration (in order to reach 100% participating mass in both loading directions), and computational time. The benefits are evident for both SPM and EEM, especially for increasing dimensions of the building.

Table 5 – Maximum axial loads in the roof bracing system diagonals and purlins – 1-portal building.

Roof brace element		CM (kN)	SPM (kN)	SPM – CM relative error (%)	EEM (kN)	EEM – CM relative error (%)
Beam 1	Diagonal	20.8	25.2	+21.2	18.8	**-9.6**
	Purlin	10.3	11.3	+9.7	15.3	+48.5
Beam 2	Diagonal	59.6	70.44	+18.2	54.4	**-8.7**
	Purlin	16.9	54.5	+332.5	22.3	+32.0

Table 6 – Maximum axial loads in the roof bracing system diagonals and purlins – 3-portal building.

Roof brace element		CM (kN)	SPM (kN)	SPM – CM relative error (%)	EEM (kN)	EEM – CM relative error (%)
Beam 1	Diagonal	18	28.7	+59.4	16.2	**-10.0**
	Purlin	8.8	16.4	+86.4	13.1	+48.9
Beam 2	Diagonal	59.3	102.1	+72.2	52.6	**-11.3**
	Purlin	17.6	64.1	+264.2	21.0	+19.3

Table 7 – Main features of the different models.
Note: results expressed as ratio between simplified model (SPM or EEM) and complete model (CM)

Parameter	1-portal building		3-portal building	
	SPM – CM Ratio (%)	EEM – CM Ratio (%)	SPM – CM Ratio (%)	EEM – CM Ratio (%)
Number of nodes	5.1	37.7	2.1	43.5
Number of elements	3.4	35.0	1.3	38.9
Number of supports	7.1	25.0	3.6	25.0
Required number of modes to reach 100% participating mass	32.1	64.3	18.0	66.0
Computational time	11.9	24.7	1.9	23.8

3.2 Industrial building with wide and irregular plan

The industrial building with wide and irregular plan considered herein is conceived as a planar extension of the building studied in the previous paragraph, with plan dimensions 300x180m. The

structural members are the same reported in **Appendix B**. **Figure 8** shows the three-dimensional view of the building.

Table 8 reports the load demand of the main structural elements of the lateral force resisting system. The data are expressed as the load demand ratio between the simplified and complete model. In the case of SPM the comparison is carried out considering the maximum values obtained in the CM for the corresponding SPM element. In the case of EEM, being the building geometry preserved, the comparison is expressed as the mean and the standard deviation considering all the corresponding CM and EEM elements.

It is important to note that EEM is suitable to account for building irregularities, as the plan irregularity which generates torsional effects. About torsional effects in planar models, different formulations are available in the literature to account for them in the seismic assessment. ASCE 41 (clause 7.2.3.2.2) states that for two-dimensional models, in the case of linear static and linear dynamic procedures, the effects of torsion shall be calculated by amplifying forces and displacement by an amplification factor. This factor, referred to as amplification multiplier for displacements, is defined for each storey as the ratio between the maximum to average diaphragm displacement. The maximum factor among different storeys should be chosen. Being such factor obtained from a three-dimensional analysis, this procedure is not suitable for SPM. Considering EN 1998-1 (clause 4.3.3.2.4.2), in the case of planar models, the torsional effects may be accounted for by amplifying the action in the individual elements by the factor δ:

$$\delta = 1 + \lambda \frac{x}{L_e} \tag{18}$$

where x is the distance of the considered element from the centre of mass of the building plan, measured perpendicularly to the planar model; L_e is the distance between the 2 outermost lateral load resisting elements, measured perpendicularly to the direction of the seismic action; λ is a coefficient varying from 0.6 to 1.2. This procedure has been applied herein to account for plan irregularities in SPM (λ =0.6).

In general, the results show a similar trend as observed in the aforementioned building with smaller plan dimensions. It is worth noting that, due to the simplified characteristics of SPM, the results are not always conservative (maximum underestimation less than 22%) especially if amplification due to torsional effects is not accounted for. Applying **Eqn.18** with $\lambda = 0.6$ leads to conservative estimates. A better correspondence is observed for EEM, which generally provides conservative results and it is suitable to include the effects of plan irregularities. The highest variation of the results is recorded in the members of the roof bracing system. It is important to note that such high variation arises especially when the roof truss system presents chord elements converging in a single node at each side of the roof truss.

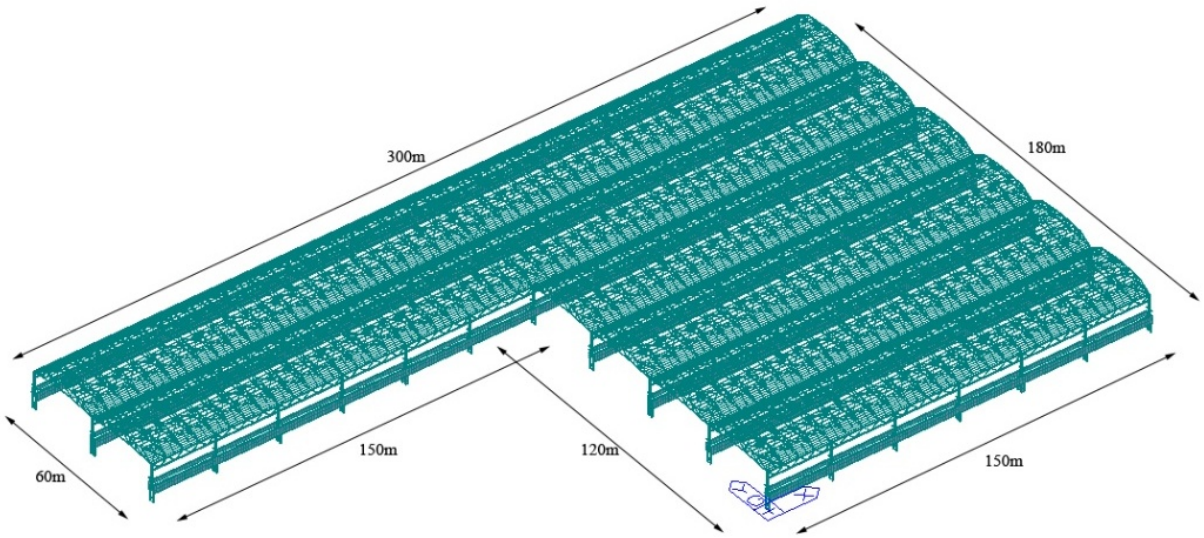

Figure 8 – 3D view of the industrial building with wide and irregular plan extension

Table 8 – Simplified and Complete models comparison.
Note: results expressed as ratio between simplified model (SPM or EEM) and complete model (CM)
** including **Eqn.18** with λ=0.6*

Element	SPM – CM ratio (%)	SPM* – CM ratio (%)	EEM – CM ratio (%)	
	Max	Max	Mean	STD
Max. shear (X-dir) on bracing column	**92.8**	125.3	**99.8**	0.3
Max. shear (Y-dir) on bracing column	**88.6**	104.1	101	2.6
Max. shear (X-dir) on standard column	107.7	145.4	**97.9**	0.2
Max. shear (Y-dir) on standard column	**85.8**	118.0	**99.9**	6.4
Max. load in the bracing column chord	**78.8**	108.4	112.6	1.8
Max. load in the bracing column diagonal	**86.9**	119.5	137.9	3.5
Load in roof beam diagonal – (Beam 1)	107.7	148.1	111.9	12.6
Load in roof beam diagonal – (Beam 2)	142.3	192.1	105.5	12.6

466 The main features of the considered models are presented in **Table 9** in terms of number of
467 elements, nodes, supports, required modes of vibration to reach 100% participating mass in both
468 loading directions and in terms of computational time. The results are expressed as the ratio
469 between the results of the simplified and the complete models. The benefits are evident for both
470 SPM and EEM.

471 *Table 9 – Main features of the different models.*
472 *Note: results expressed as ratio between simplified model (SPM or EEM) and complete model (CM)*

Parameter	SPM – CM Ratio (%)	EEM – CM Ratio (%)
Number of nodes	0.8	43.3
Number of elements	0.5	38.8
Number of supports	1.5	25.0
Required number of modes to reach 100% participating mass	3.3	58.7
Computational time	0.5	24.1

473 ## *4 Conclusions*

474 The paper investigates the suitability of simplified building models as advanced screening tools
475 for a first estimate of the seismic vulnerability assessment of the lateral force resisting system of
476 older and large industrial buildings. The considered buildings are characterised by a wide extension
477 and by a structural layout typical of pre- and post- World War II, widespread over the Italian
478 territory. Such buildings present a general low ductility of the connections and the absence of
479 capacity design provisions. In the case of wide industrial buildings, extensive industrial areas or
480 large portfolios, seismic screening procedures can provide a quick evaluation for the seismic risk
481 assessment and management, as required in industrial and insurance fields. Therefore, two
482 simplified building models are developed and evaluated: Simplified Planar Model (SPM) and
483 Equivalent Elements Model (EEM).

484 In SPM the seismic loads acting on the lateral force resisting system are determined by means of
485 response spectrum analyses on simplified finite element planar models. The in-plane longitudinal
486 model considers the columns connected to the lateral bracing and half bay of the framing beams and
487 crane runway beams. Sets of additional springs and masses account for both the stiffness and the
488 mass of the portions of the building which are not directly modelled. The out-of-plane transverse

489 model is represented by a column with its tributary mass (at the roof and at the crane levels) for
490 cantilever columns pin-connected to the roof truss, or by half the portal in the case of portal frames.
491 In EEM, a three-dimensional finite element model of the building is defined by means of
492 equivalent beam elements to reduce the number of degrees of freedom and the computational effort.
493 Equivalent elements are introduced in lieu of columns, laced members and battened members with
494 parallel chords. Elastic response spectrum analyses are conducted. The loads on the real structural
495 elements are obtained in a simplified manner by assigning the resulting axial load and bending
496 moment to the chords of the original elements, while the load on the diagonal elements are obtained
497 from the equilibrium with the equivalent element shear.
498 Both SPM and EEM have been applied to selected case studies resembling industrial steel
499 buildings with a structural layout compatible with the investigated building typology. The results of
500 such application show the suitability of the proposed procedures as advanced seismic screening
501 tools able to provide a first estimate of the loads in the members of the lateral force resisting
502 system. A significant reduction of the computational effort is also recorded. The SPM procedure is
503 the most suitable for a quick and preliminary seismic assessment of the lateral force resisting
504 system. In the case of buildings with significant plan irregularities higher differences are observed.
505 In such conditions the building three-dimensional model should be considered. The EEM procedure
506 captures the variation of loads among the elements, being the building geometry preserved in the
507 simplified model. The proposed building models are suitable to highlight potential seismic
508 deficiencies and can be adopted both to rank the seismic vulnerability of buildings among a
509 portfolio and to get a preliminary idea of the seismic risk of a given building. Likewise any seismic
510 screening tool, additional and refined analyses are required to confirm the deficiencies found and to
511 demonstrate the adequacy of the structure.
512

References

ABAQUS user's manual version 6.11 (2011) Dassault Systemes Simulia Corp

AASHTO (2009), Guide specifications for LRFD seismic bridge design, Washington, D.C.

ASCE/SEI 41 (2014), Seismic evaluation and retrofit of existing buildings, American Society of Civil Engineers, Reston, Virginia, USA

Ballio G, Mazzolani FM (1983), Theory and Design of Steel Structures, Chapman and Hall, London.

Belleri A, Brunesi E, Nascimbene R, Pagani M, Riva P (2014), Seismic Performance of Precast Industrial Facilities Following Major Earthquakes in the Italian Territory. *J. Perform. Constr. Facil.*, doi:10.1061/(ASCE)CF.1943-5509.0000617

Belleri A, Torquati M, Riva P, Nascimbene R (2015), Vulnerability assessment and retrofit solutions of precast industrial structures. *Earthquake and Structures*, **8**(3):801-820 doi:10.12989/eas.2015.8.3.801

Building Seismic Safety Council (BSSC) (2003), NEHRP recommended provisions for seismic regulations for new buildings and other structures (FEMA 450), Washington, D.C.

CEN (2004) EN 1998-1:2004, Eurocode 8: Design of structures for earthquake resistance - Part 1: General rules, seismic actions and rules for buildings. European Committee for Standardization, Brussels, Belgium.

CEN (2005) EN 1998-3:2005, Eurocode 8: Design of structures for earthquake resistance - Part 3: Assessment and retrofitting of buildings. European Committee for Standardization, Brussels, Belgium.

Chopra AK, Goel RK (2002), A modal pushover analysis procedure for estimating seismic demands for buildings. *Earthq. Eng. Struct. Dyn.*, **31**(3), 561-582.

D.M. 14/01/2008, Italian Building Code (2008) - Norme tecniche per le costruzioni. (in Italian).

FEMA 154 (2002) Rapid Visual Screening of Buildings for Potential Seismic Hazards: A Handbook, Second Edition, Washington DC, USA

FEMA 356 (2000), Prestandard and commentary for the seismic rehabilitation of buildings. Federal Emergency Management Agency Washington, D.C.

HAZUS (2003). *HAZUS-MH®MR4 Technical Manual*, Federal Emergency Management Agency (FEMA)

Kreslin M, Fajfar P (2011), The extended N2 method taking into account higher mode effects in Elevation. *Earthq. Eng. Struct. Dyn.*, **40**(14), 1571-1589.

Liberatore L, Sorrentino L, Liberatore D, Decanini LD (2013), Failure of industrial structures induced by the Emilia (Italy) 2012 earthquakes, *Eng. Fail. Anal.*, **34**, 629-647.

López-Almansa F, Montaña MA (2014), Numerical seismic vulnerability analysis of mid-height steel buildings in Bogotá Colombia. *Journal of Constructional Steel Research*, **92**, 1–14.

Magliulo G, Ercolino M, Petrone C, Coppola O, Manfredi G (2014), Emilia Earthquake: the Seismic Performance of Precast RC Buildings, *Earthquake Spectra*, **30**(2), 891-912.

MidasGEN 2012 (v3.1), MIDAS Information Technologies Co. Ltd

Nguyen AH, Chintanapakdee C, Hayashikawa T (2010), Assessment of current nonlinear static procedures for seismic evaluation of BRBF buildings. *Journal of Constructional Steel Research*, **66**, 1118–1127.

Petruzzelli F (2013), Scale-dependent procedures for seismic risk assessment and management of industrial building portfolios, PhD Thesis, University of Naples Federico II

Petruzzelli F, Della Corte G, Iervolino I (2012a), Seismic Risk Assessment of an Industrial Steel Building. Part 1: Modelling and Analysis. Proceedings of the 15th World Conference on Earthquake Engineering, Lisboa, PT, Paper No.3086.

Petruzzelli F, Della Corte G, Iervolino I (2012b), Seismic Risk Assessment of an Industrial Steel Building. Part 2: Fragility and failure Probabilities. Proceedings of the 15th World Conference on Earthquake Engineering, Lisboa, PT, Paper No.3088.

Pitilakis K, Argyroudis S, Kakderi K, Argyroudi A (2013), Systemic Seismic Vulnerability and Risk Analysis for Buildings, Lifeline Networks and Infrastructures Safety Gain, European Commission, ISBN 978-92-79-33135-0

Roeder CW, MacRae GA, Scott K (2002), Seismic performance of older steel frame mill buildings. *Journal of Constructional Steel Research*, **58**, 759–777

Vamvatisikos D, Cornell CA (2002), Incremental dynamic analysis. *Earthq. Eng. Struct. Dyn.*, **31**(3), 491-514.

Wijesundara KK, Nascimbene R, Rassati GA (2014), Modeling of different bracing configurations in multi-storey concentrically braced frames using a fiber-beam based approach, *Journal of Constructional Steel Research*, **101**, 426-436.

APPENDIX A

In the case of compressive seismic loads, it is important to evaluate buckling of single elements and buckling of sets of elements, particularly for those members designed for tensile loads. The loads obtained from the simplified seismic analyses need to be compared to the buckling load of the members. Considering for instance the roof of industrial single-storey steel buildings, the typical design practice neglects the stiffening contribution of the roof panels. Roof braces are in charge of distributing horizontal seismic loads between adjacent frames and to provide restraint against buckling of the compressed chord of roof trusses. In the case of buckling of the roof braces such transferring and stabilizing function is jeopardized and the roof truss could buckle as a consequence of seismic compressive loads. Analysing in detail the roof truss shown in **Figure A1**, constituted by double-L profiles (outer chord 110x110x10mm, inner chord 90x90x9mm, truss web 60x60x6mm), the compression arising in the inner chord during an earthquake could lead to its instability if no lateral restraints are provided. Such phenomenon could cause the roof failure and therefore it needs to be dealt with and eventually avoided.

It is worth noting that the buckling load (F_b) is dependent both on the stiffness of the roof diaphragm and on the vertical load (N) transferred by each purlin. Considering **Figure A1**, in the case of rigid roof diaphragm the buckling mode involves the inner chord of the roof truss, while without roof diaphragm (i.e. in the case of failure of the roof bracing elements) the buckling mode involves both the inner and outer chords and it is characterized by a lower value.

As regards the influence of the vertical load N (**Figure A2**), it is observed how the effectiveness of the roof diaphragm leads to increasing buckling loads for increasing values of N. Indeed, higher vertical loads lead to higher tension in the bottom chord which needs to be overcome by higher compressive loads before buckling occurs. The results shown in **Figure A1** and **Figure A2** are obtained from post-buckling analyses (Abaqus 2011) with a out-of-plane imperfection (L/500, being L the truss length) corresponding to the first buckling mode in the rigid diaphragm case. The

599 rigid diaphragm conditions are obtained from placing out-of-plane restraints at the joints of the
600 outer chord.

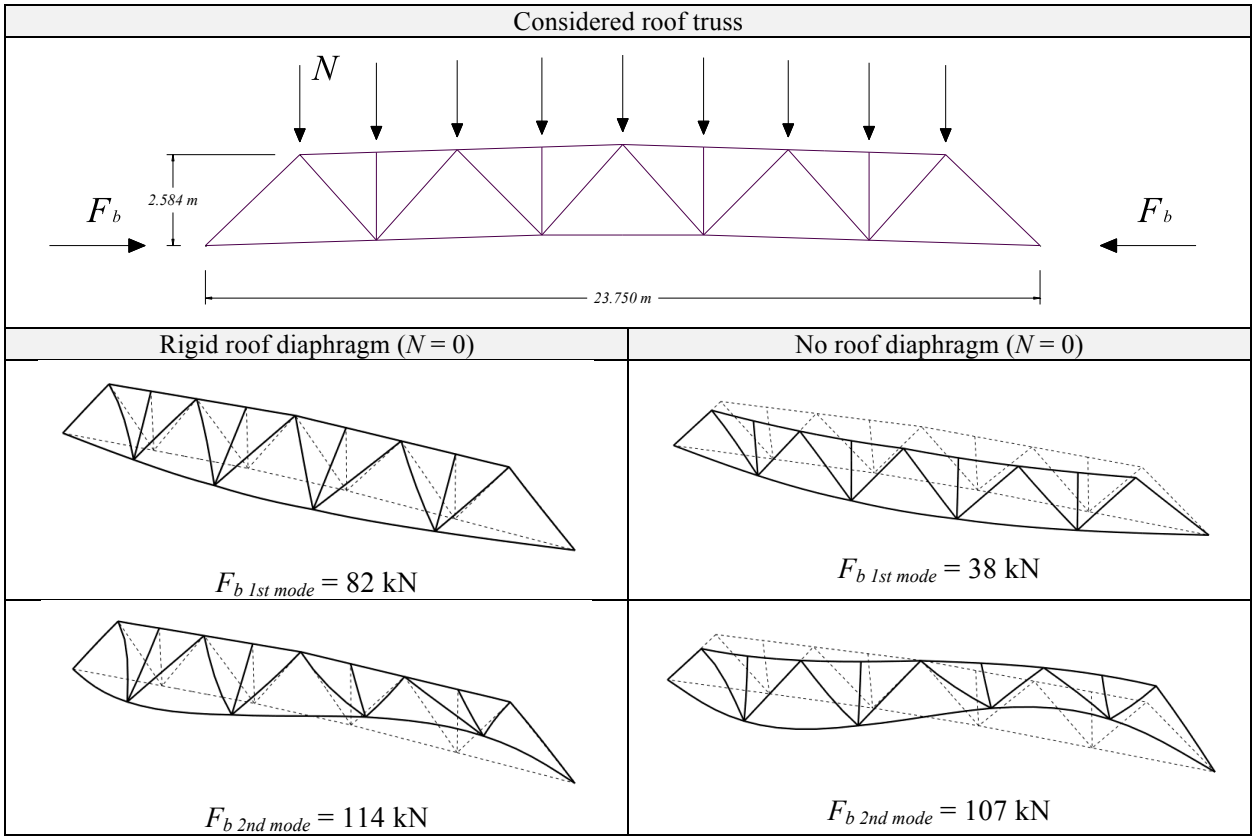

601 *Figure A1 – Buckling load as a function of roof diaphragm stiffness*
602

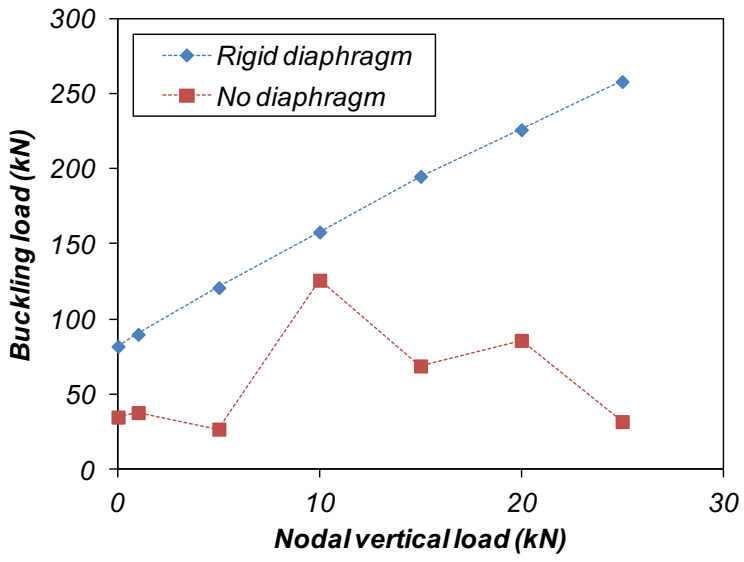

603

604 *Figure A2 – Buckling load as a function of gravity load transferred by purlins (N)*
605

606 ## *APPENDIX B*

607 **Table B1**, **Table B2** and **Table B3** contain the geometry of the members and the corresponding
608 equivalent elements adopted in the validation of the proposed procedure. Properties are defined
609 with reference to equations 1-17.

610 *Table B1 – Details of the columns and of the corresponding equivalent elements*

Columns	ID	Section	Equivalent Element	ID	Properties
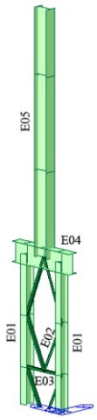 Standard column	E01	HEA 360	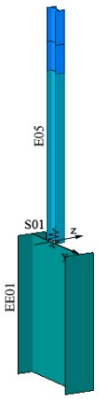	EE01	h = 3.490 m B = 1.204 m t_w = 0.0007 m t_f = 0.0022 m ρ_{eq} = 463 kN/m^3
	E02	2L 90x90x9			
	E03	2L 80x80x9			
	E04	I 400x740		S01	$k_{R,y}$ = 752 kN m/rad $k_{R,z}$ = 1590000 kN m/rad
	E05	I 400x600			
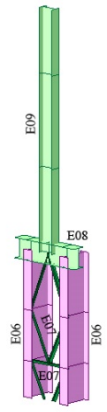 Bracing column	E06	I 400x1100	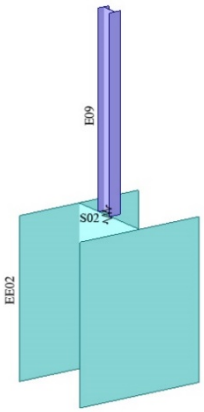	EE02	h = 3.222 m B = 4.437 m t_w = 0.0013 m t_f = 0.0019 m ρ_{eq} = 513 kN/m^3
	E07	2L 100x10			
	E08	I 500x750		S02	$k_{R,y}$ = 1440 kN m/rad $k_{R,z}$ = 1890000 kN m/rad
	E09	I 400x600			

611 *Table B2 – Details of the crane running beams and of the corresponding equivalent elements*

Crane beams		Equivalent element	
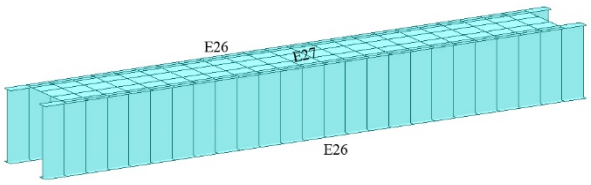		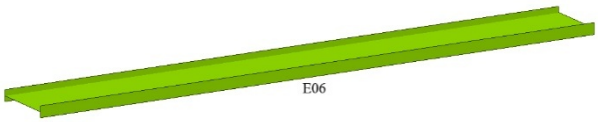	
Element ID	Section	ID	Properties
E26	I 480x3000	EE06	H = 2.800 m B = 0.480 m t_w = 0.006 m t_f = 0.106 m ρ_{eq} = 77 kN/m^3
E27	Plate thickness 6 mm		

612

613

614 *Table B3 – Details of the roof supporting trusses and of the corresponding equivalent elements*

Longitudinal supporting truss		Equivalent element	
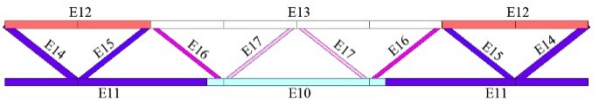		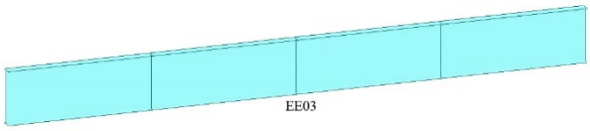	
ID	Section	ID	Properties
E10	Box 325x10	EE03	H = 2.260 m B = 0.4491 m t_w = 0.0013 m t_f = 0.0212 m ρ_{eq} = 85 kN/m^3
E11	Box 325x7.1		
E12	Box 325x6.3		
E13	Box 325x8		
E14	Box 285x155x6.3		
E15	Box 220x7.1		
E16	Box 155x115x4		
E17	Box 135x4		

Transversal supporting truss	ID	Section
	E20	Box 175x5
	E21	Box 135x5.6
	E22	Box 175x7.1
	E23	Box 90x3.6
	E24	Box 135x3.6
	E25	Box 135x3.2

615 *Table B4 – Details of the roof and of the corresponding equivalent elements*

Roof beams		Equivalent element	
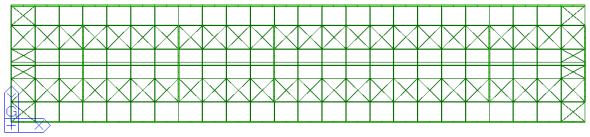		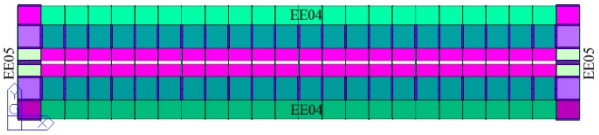	
Element	Section	ID	Properties
Diagonals	L70x5	EE04	H = 6.123 m B = 0.035 m t_w = 0.00021 m t_f = 0.035 m ρ_{eq} = 142.0 kN/m^3
Purlins	C100x160x3	EE05	H = 6.250 m B = 0.064 m t_w = 0.00014 m t_f = 0.064 m ρ_{eq} = 65.17 kN/m^3

616